Inherent envelope fluctuations in forward masking: Effects of age and hearing loss.

Marc A. Brennan[1], Adam Svec[2], Afagh Farhadi[3], Braden Maxwell[3], & Laurel H. Carney[3]

[1]University of Nebraska-Lincoln, Lincoln, NE 68583

[2]San José State University, San Jose, CA 95192

[3]University of Rochester, Rochester, NY 14642

Correspondence:

Marc Brennan

University of Nebraska-Lincoln

4075 East Campus Loop

Lincoln, NE 68583

Fax: 402 472 3814

Phone: 402 472 3132

Email: Marc.Brennan@unl.edu

ABSTRACT

Forward masking is generally greater for Gaussian noise than for low-fluctuation noise maskers, i.e., GN disruption. Because the minimal hearing loss that is associated with older age may affect GN disruption differently than more significant hearing loss, the current study explored the contribution of minimal hearing loss associated with older age to GN disruption. GN disruption was measured using three masker-signal delays (25, 75, and 150 ms) for three adult participant groups: younger participants with normal hearing, older participants with minimal hearing loss, and older participants with sensorineural hearing loss. The role of underlying mechanisms was tested using a computational model for midbrain neurons. The primary result suggests that older listeners with mild threshold elevations that typically occur with age may be more susceptible to the deleterious effects of masker-envelope fluctuations than younger listeners with normal hearing. Results from the computational model suggest that there may be a larger influence of efferent feedback and saturation of inner hair cells on forward masking and GN disruption than previously expected.

Keywords: aging, hearing loss, forward masking, auditory model

Abbreviations: Auditory Nerve (AN), Auditory Nerve Fiber (ANF), equivalent-rectangular bandwidth (ERB_N), Gaussian noise (GN), inferior colliculus (IC), inner hair cell (IHC), low-fluctuation noise (LFN), low/high-spontaneous rate (L/HSR), Medial Olivocochlear (MOC), normal hearing (NH), outer hair cell (OHC), older participants with minimal hearing loss (OMHL), older participants with sensorineural hearing loss (OSNHL), same-frequency inhibition-excitation (SFIE), sensorineural hearing loss (SNHL), younger participants with normal hearing (YNH).

I. INTRODUCTION

The temporal envelope of Gaussian noise (GN) contains short-term fluctuations in level. As the bandwidth of GN decreases, these fluctuations tend to increase the amount of masking for both simultaneous maskers (Pumplin, 1985; Zurek and Durlach, 1987; Hartmann and Pumplin, 1988; Kohlrausch *et al*., 1997; Savel and Bacon, 2003) and forward maskers (Moore, 1981; Svec *et al*., 2015, 2016) relative to a masker of equivalent bandwidth and level, for which the temporal envelope fluctuations have been minimized, referred to here as low-fluctuation noise (LFN). Given that less forward masking is generally expected and observed for LFN than for GN (e.g., Svec *et al*., 2015, 2016), the additional masking attributed to the envelope fluctuations is often assessed by subtracting the LFN threshold from the GN threshold, referred to here as GN disruption. Considering that masker fluctuations contribute negatively to speech recognition (Stone *et al*., 2011, 2012), the mechanisms that contribute to GN disruption have implications for understanding the processes that contribute to the speech recognition difficulties often experienced by listeners in noisy situations (Füllgrabe *et al*., 2015; Brennan *et al*., 2016). The purpose of this study was to ascertain plausible mechanisms that contribute to GN disruption as a function of age and hearing status. To accomplish this, GN disruption at three different masker-signal delays was assessed for younger normal hearing (YNH), older participants with minimal hearing loss (OMHL), and older participants with sensorineural hearing loss (OSNHL).

A. Cochlear Compression and Listener Uncertainty

Cochlear compression and listener uncertainty could play a role in GN disruption. For participants with SNHL, a linearized cochlear response should yield larger effective amplitude

peaks than a compressive cochlear response (NH), which would likely yield greater GN disruption. These larger effective amplitude peaks may result in an increased potential for confusing an amplitude fluctuation near the end of the masker for the onset of the brief signal, referred to as either listener uncertainty or the "confusion effect" (Moore, 1981; Moore & Glassberg, 1985; Neff, 1986). However, such an explanation conflicts with 1) the greater GN disruption, for a 25 ms masker-signal delay, that occurred for OMHL relative to both YNH and OSNHL participants by Svec *et al*. (2015) and 2) the greater GN disruption observed by Svec *et al*. (2016) for OSNHL relative to YNH participants for a 75-ms masker-signal delay—a delay time for which confusion effects should no longer occur. As elaborated below, one potential reason for the greater GN disruption for the OMHL participants in Svec *et al*. (2015) was that these participants had slightly higher hearing thresholds (i.e., minimal hearing loss) than the YNH participants.

B. Inhibition at the Inferior Colliculus

Multiple peripheral and central processes, such as the middle-ear muscle reflex, neural adaptation, efferent innervation from the medial olivocochlear bundle, and dynamic range adaptation could also contribute to forward masking and, by extension, to GN disruption (See a review by Jennings, 2021). Nelson *et al*. (2009) argued that single auditory-nerve fibers (ANFs) tuned to the frequency of the signal cannot account for forward masking due to a limited dynamic range of discharge rates and maximum threshold shifts, two attributes of ANF responses (in anesthetized animals) that do not mirror psychophysical forward-masking results. After measuring recovery from forward masking at the level of the inferior colliculus (IC) in awake marmosets, Nelson and colleagues asserted that the phenomenon of forward masking is likely a consequence of inhibitory neural responses arising between the auditory nerve and the IC. While it remains

unclear whether these inhibitory responses differ between GN and LFN, recent physiological work has suggested that GN disruption for tone-in-noise stimuli is observable from extracellular recordings of IC cells in awake rabbits (Fan *et al*., 2021).

C. Medial Olivocochlear Efferent System

The Medial Olivocochlear (MOC) efferent system could play a role in GN disruption. The MOC system provides efferent input to the outer hair cells (OHCs) that regulates OHC electromotility. Increased MOC activity is associated with decreased OHC electromotility and, in turn, reduced cochlear gain and smaller vibrations on the basilar membrane (Fuchs and Lauer, 2019). Upward shifts of 2-14 dB of auditory-nerve rate-level functions with electrical stimulation of the MOC have been observed (Gifford and Guinan, 1983), with the largest shifts occurring for levels between 45and 75 dB SPL (Guinan, 2018). The MOC efferent system receives ascending inputs from peripheral auditory neurons, as well as descending projections from the IC and other more central auditory structures (Mulders and Robertson, 2000; Schofield, 2011). While the cumulative contribution of the MOC to auditory physiology and perception remains unclear (e.g., Jennings, 2021), Carney (2018) argued that one purpose of the MOC efferent pathway might be to regulate OHC gain to control the saturation of inner hair cells (IHCs), thereby preserving cross-CF contrast in low-frequency temporal fluctuations in ANF responses, referred to as neural fluctuations. Due to the fact that IC neurons are sensitive to envelope fluctuations (reviewed in Joris *et al*., 2004) and the IC includes descending projections to the MOC, Carney additionally argued that neural fluctuations may excite MOC efferents and decrease OHC electromotility, leading to reduced cochlear gain. Farhadi *et al*. (2021) modeled IC firing rate as a function of time in response to amplitude-modulated stimuli. The results suggested that predictions were not

accurate without the inclusion of efferent-regulated cochlear gain driven by IC inputs to the MOC system, providing additional support for the assertion that fluctuating inputs to the IC are likely directly affecting MOC spike rates, and in turn, cochlear gain. According to the computational model of Farhadi *et al*. (2021), the effect of this decreased cochlear gain in response to a fluctuating input, such as GN, should be decreased IHC saturation, and thus greater ANF fluctuations.

Decreased cochlear gain following stimulus presentation begins to decay within 25 ms of the masker offset (Roverud and Strickland, 2010), but appears to remain, in diminished form, up to 50 s following stimulus presentation (Brown, 2001; Cooper and Guinan, 2003). This initial time course of decreased cochlear gain following stimulus presentation shares correspondence with the time course of recovery for forward masking, with an exponential decay in masking that extends from 0 to approximately 128 ms following masker offset (e.g., Jesteadt *et al.,* 1982). If cochlear gain is influenced by temporal-envelope fluctuations through IC projections to the MOC, masker envelope fluctuations associated with a GN forward masker should induce a reduction in cochlear gain and a concomitant decrease in the response of the IC to the signal that temporally follows a masker stimulus. Consequently, the decrease in masking associated with longer masker-signal delays would be expected to follow the time course of decreased cochlear gain following stimulus presentation, primarily from 25 to 125 ms (Brown, 2001; Cooper and Guinan, 2003; Roverud and Strickland, 2010; Rabbitt and Brownell, 2011). In contrast, when the IC receives relatively small fluctuations (e.g., produced by LFN), the IC projections to the MOC should induce less cochlear-gain reduction relative to a stimulus with larger fluctuations (e.g., GN). The net effects would likely result in a higher IC rate in response to a signal following a LFN masker than following a GN forward masker, which is consistent with GN disruption. These effects of the MOC efferent

system could account for the gradual decrease in GN disruption observed with increasing masker-signal delay (25, 50, and 75 ms) for participants with NH (Svec *et al.,* 2016).

Additional important factors moderating the MOC influence on GN disruption are: a) the *relative* degree of IHC saturation in response to the GN and LFN forward maskers; and b) changes in MOC physiology associated with age and SNHL. As described above, IHC saturation determines the neural fluctuations in response to these two types of maskers. The relative IHC saturation in response to these maskers, and thus the neural fluctuations and the MOC responses that they elicit, would be expected to vary across groups of participants. For younger participants with audiometric thresholds within normal limits, IHCs will tend to saturate in response to both GN and LFN forward maskers when presented at high sound levels, resulting in a relatively small amount of predicted GN disruption for moderate and high-level maskers. For older participants with slightly elevated audiometric thresholds (e.g., small amounts of hearing loss), less IHC saturation would be expected. Although the influence of older age on the MOC efferent system is unclear (Fuchs & Lauer, 2019), neural fluctuations and changes in cochlear gain would still be expected, which together may result in relatively large GN disruption for older participants with small amounts of hearing loss relative to participants with better hearing. For participants with significant SNHL, two factors may affect the magnitude of GN disruption. First, even when masker presentation levels are high, IHCs might not saturate for either GN or LFN maskers due to threshold elevation. Second, the impact of the MOC efferent system on cochlear gain is reduced (Carney, 2018; Fuchs and Lauer, 2019). Consequently, less GN disruption would be expected for older participants with substantial SNHL than for older participants with minimal hearing loss. After an initial cochlear-gain decrease associated with an input stimulus, an intact MOC system allows cochlear gain to increase during the interval from 25 to 125 ms or more after stimulus offset

(Brown, 2001; Roverud and Strickland, 2010), implying that differences in GN disruption for YNH, OMHL, and OSNHL should be maximal at a short masker-signal delay and decrease for longer masker-signal delays.

D. Research Questions

To clarify possible physiological mechanisms associated with GN disruption, the current study examined the effects of age and SNHL on forward-masked thresholds when presented with maskers with relatively large (GN) or relatively small (LFN) fluctuations in level over time. Masked thresholds were obtained for a 4000-Hz pure-tone signal when presented after the offset of GN or LFN maskers at three masker-signal delays (25, 75, and 150 ms) for YNH, OMHL, and OSNHL participants. Contributions of inhibition and MOC efferent system to GN disruption were evaluated using a computational model of midbrain neurons. The following hypotheses were formed:

1) If a lack of cochlear compression strongly contributes to GN disruption (e.g., by increasing the effects of uncertainty), then GN disruption should be greatest for the OSNHL participants, less for OMHL participants and least for YNH participants.
2) If differences in the physiological response of the MOC efferent system for GN and LFN maskers strongly contribute to GN disruption, then GN disruption should vary non-monotonically with audiometric threshold at the signal frequency. The most GN disruption is hypothesized to occur for participants with relatively small amounts of hearing loss (OMHL participants), for whom IHC saturation and neural fluctuations would differ the most between the two masker types. Additionally, a computational model incorporating

the MOC efferent system should better predict GN disruption than a model without the MOC efferent system.

For all mechanisms that contribute to GN disruption, differences in GN disruption for each group were hypothesized to decrease as the masker-signal delay increased.

II. METHODS

A. Participants

A total of 57 participants were enrolled in this study. Five participants were excluded because they did not qualify based on their hearing thresholds (see below). Of the remainder, 18 YNH (19 – 25 years, M=22), 14 OMHL (65 – 81 years, M=71), and 20 OSNHL (62 – 82 years, M=71) participants completed the study. Within each group, the age of the participants was evenly distributed across their respective age ranges. A graduate student in audiology measured hearing thresholds (ANSI, 2004) for all participants using conventional audiometry (ASHA, 2005) at 6000 Hz and at octave frequencies from 250 to 8000 Hz. Hearing thresholds for the test ear are plotted in Fig. 1. Hearing thresholds for the non-test ear were within 15 dB of those for the test ear as measured by pure tone average (500, 1000, 2000 Hz). NH was defined as hearing thresholds less than 30 dB HL from 250 to 4000 Hz. However, one OMHL participant with a hearing threshold of 30 dB HL at 500 Hz participated. SNHL was defined as air conduction thresholds from 35 to 65 dB HL at 4000 Hz and, for frequencies with hearing loss greater than 25 dB HL, bone conduction thresholds within 10 dB of the air conduction threshold. Participants who did not have NH, SNHL outside the range of 35 to 65 dB HL at 4000 Hz, or a 25 dB or greater difference in air-conduction thresholds between the two ears at 4000 Hz did not qualify. All subjects were native

English speakers. Data were collected at the University of Nebraska-Lincoln. Approval for this study was obtained from the Institutional Review Board. Participants consented to join the study and were paid for their time.

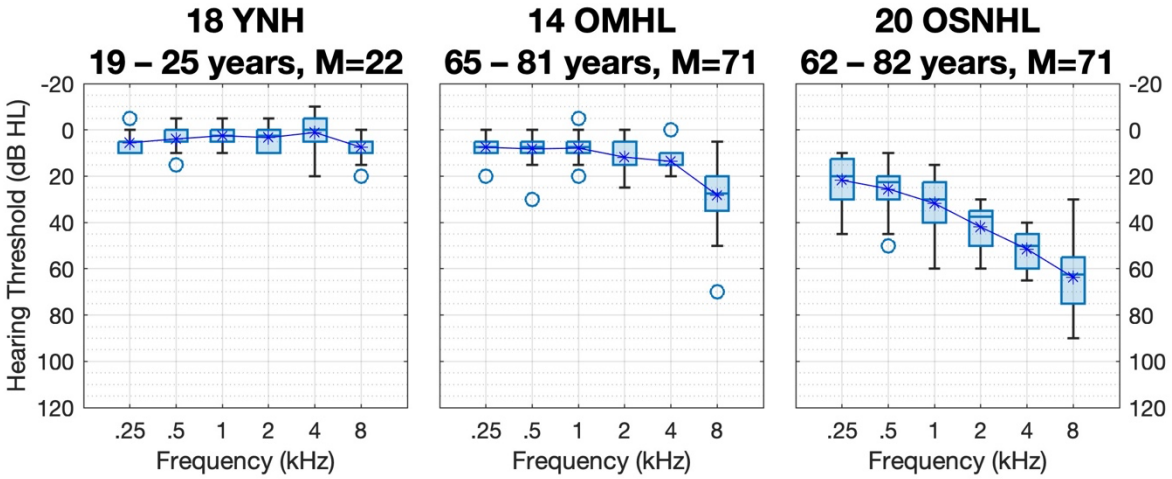

Fig. 1. (color online) Plots of hearing threshold for each participant group. Number of participants, age range, and median age are also provided. For this and the remaining box and whisker plot, each box represents the interquartile range, each line represents the median, each asterisk represents the mean, each circle represents an outlier (>1.5 times the interquartile range), and whiskers represent the most extreme value that is not an outlier.

B. Stimuli and Apparatus

Stimuli were generated using a personal computer (22.05 kHz sampling rate; 16 bits per sample) and custom MATLAB (2019a) scripts. All durations were measured from the 0-amplitude points of the onset and offset ramps. Using the formula provided by Glasberg and Moore (1990), maskers were one-third equivalent rectangular bandwidth (1/3 ERB_N) centered at 4000 Hz (Glasberg and Moore, 1990). Maskers were 400 ms in duration, including 5-ms cosine-squared

ramps. LFN was generated using a Hilbert transform (Buss *et al.,* 2006) with the PsyAcoustX package (Bidelman *et al*., 2015). Specifically, the Hilbert envelope was computed for each 1/3 ERB_N GN generated. Each GN was divided in the time domain by its Hilbert envelope and then multiplied by the original spectrum in the frequency domain; these last two steps were repeated ten times to yield the final version of LFN.

Stimuli were calibrated using a 6-cc flat plate coupler and a Larson Davis System 824 sound level meter (Depew, New York). Signal levels are reported as the root-mean-square peak equivalent (0.707 x peak pressure) in dB SPL. The signal was a 4000-Hz pure tone, 10 ms in duration including 5-ms cosine-squared ramps. The signal was presented either without the masker (quiet condition) or with the signal onset 25, 75, or 150 ms after the masker offset (masker conditions). Each stimulus interval was preceded by 400 ms of silence and then followed by 400 ms of silence and, for each condition, interval durations were equivalent. The 24-bit digital stimuli were converted to analog (RME Babyface sound card, Haimhausen, Germany), amplified by a HeadAmp 4 Pro headphone distribution amplifier (Baton Rouge, Louisiana), and presented to one ear using Sennheiser HD-25 headphones (Wedemark, Germany). All testing took place in a single-walled sound attenuated room, with each participant sitting in front of a touch-screen monitor.

C. Procedures

For all experimental conditions, the signal level was varied adaptively to estimate the threshold corresponding to 71% correct with a two-down, one-up rule (Levitt, 1971). For all masker conditions, the masker level was fixed at 80 dB SPL. To ensure audibility of the signal for the OSNHL participants, the starting level of the signal was 80 dB SPL. The initial step size of 18 dB was reduced to 9 dB after the first reversal and 6 dB after the second reversal. Then, a step size

of 3 dB was used. Data collection ended after a total of nine reversals. The minimum signal presentation level was -10 dB SPL, and the maximum signal presentation level was 90 dB SPL. None of the participants had tracks with 3 presentation levels in a row at 90 dB SPL (i.e., none were at ceiling). The average of levels at the last four reversals was taken as the threshold.

A trial consisted of three observation intervals separated by 300 ms. Each interval was marked by a separate button which was illuminated on the touchscreen monitor for the stimulus duration including the encapsulating silence of 400 ms, for approximately 1200 ms per interval. For the absolute-threshold condition, one randomly selected interval contained the signal. For the masker conditions, one randomly selected interval contained the masker and signal, and the other two contained only the masker. Participants indicated the interval which they believed contained the signal by pressing the corresponding button and feedback was provided. For each condition, threshold was measured three times and the final threshold was recorded as the average across the three measurements. Threshold for the absolute-threshold condition was measured first followed by the masker conditions in random order.

D. Computational Models

Computational models for auditory-nerve (AN) and midbrain responses were used to provide insight into mechanisms that possibly contribute to GN disruption. All models included stages for the cochlea, auditory-nerve fibers, and inferior colliculus (Zilany et al., 2014; Nelson and Carney, 2004). One model was an updated version of the Zilany and colleagues' model that also included MOC efferents (Farhadi *et al*., 2021). Figures 2 and 3 provide overviews of the Farhadi *et al*. model, where firing rates are depicted for one trial of each masker type for a hearing

threshold of 15 dB HL at 4 kHz (i.e., an OMHL participant). The computational model is publicly available for download at https://DOI.org/10.17605/OSF.IO/AJVWD.

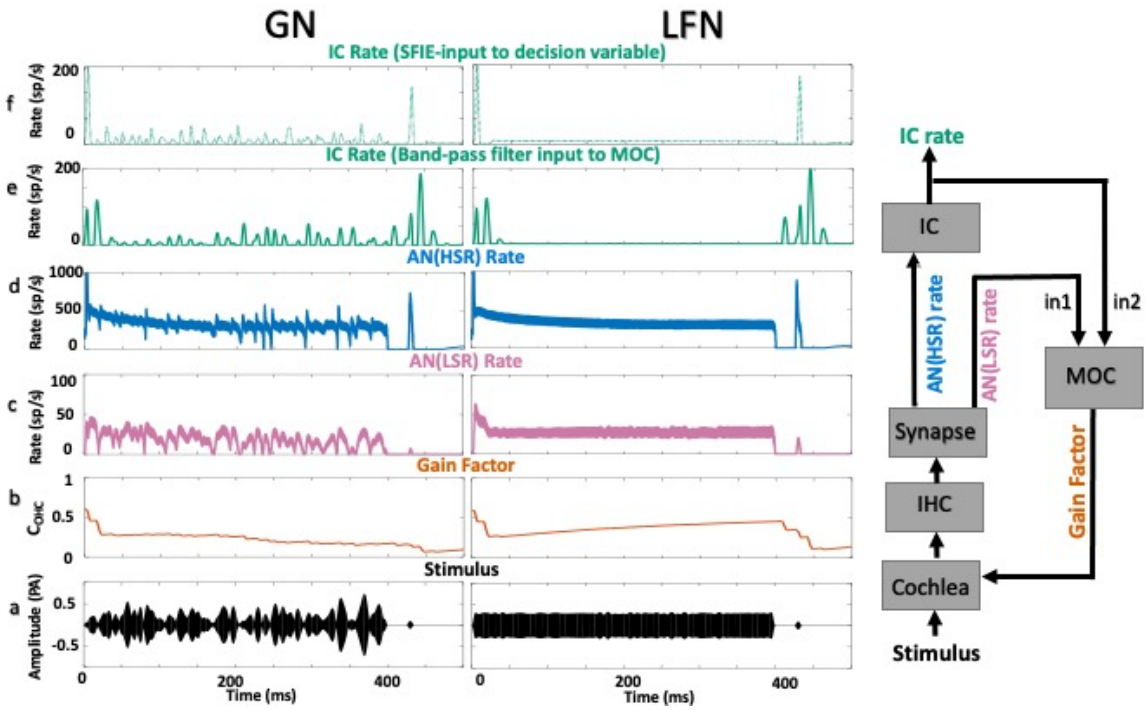

Fig. 2. (color online). Computational model including MOC efferent system. Showing example simulation of one frequency channel for OMHL. a) GN and LFN stimuli at the input to the model ultimately result in b) cochlear gain factors that vary throughout the stimulus. c) Low-spontaneous rate (LSR) and d) high-spontaneous rate (HSR) AN responses are the instantaneous-rate functions at the output of the model synapse (right). e) Model IC response of band-pass filter model. The LSR fiber was used to represent wide-dynamic-range responses from the cochlear nucleus, which were combined with the IC model response as inputs to the MOC stage (right). Larger fluctuations in the IC response to GN stimuli resulted in greater gain reduction throughout the GN masker as compared to the LFN masker. Therefore, the peak rate in response to the signal for the HSR fiber was reduced after the GN masker as compared to the LFN masker. e) Subsequently, for the IC

SFIE response that was the input to the decision variable, the relative rates of the signal to masker was smaller for GN compared to LFN. CF = 4 kHz. The signal was 70 dB SPL.

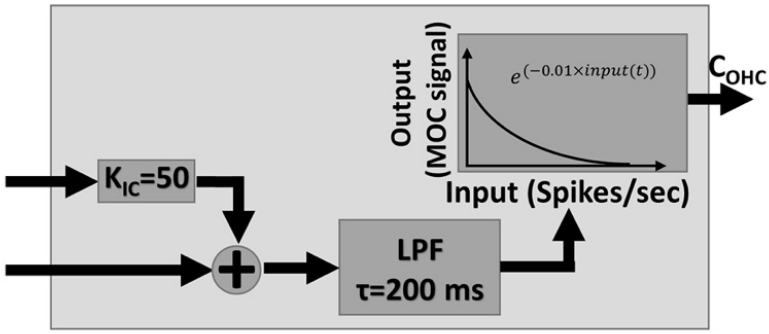

Fig. 3. Computational model of MOC efferent system. Depicts mapping of input spike rate to MOC gain factor to cochlea. Input spike rate from IC was scaled and added to that from a LSR auditory-nerve fiber, low-pass filtered, and then converted to MOC gain factor. Higher MOC spike rate resulted in smaller gain factor.

Both sets of computational models (with and without efferents) incorporated physiological properties including the saturation of IHC transduction and synaptic saturation and adaptation. Peripheral tuning of these models was based on data for human participants (Ibrahim and Bruce, 2010). Both computational models included lowpass filters corresponding to the outer and inner hair cells, each with adjustable scaling factors. Decreasing the value of the computational model parameter C_{OHC} (max=1, min=0) reduced cochlear gain, while decreasing the value of C_{IHC} reduced sensitivity of the IHC and increased the dynamic range (i.e., pushed the saturation point of the IHC nonlinearity to higher input levels). The initial C_{OHC} and C_{IHC} scaling factors were set to match the mean audiometric threshold in dB HL for each participant group. Two-thirds of the threshold shift was ascribed to OHC, based on acoustic trauma observed in cats (Bruce *et al.,* 2003; Zilany and Bruce, 2007) and estimated OHC integrity in humans with SNHL (Plack *et al.,* 2004).

The model that included the MOC efferents (Farhadi *et al*., 2021) incorporated implementations of low- and high-spontaneous rate fibers (LSR, HSR) in different roles. Because the input to the ascending pathway to the IC is dominated by HSR fibers (Carney 2018), the HSR fibers provided input to the brainstem/IC model, which in turn provided one of two descending neural inputs to the MOC. The other input to the MOC consisted of afferent LSR fibers, reflecting the physiological observation that inputs to the MOC have wide dynamic ranges (Ye *et al*., 2000). Together, these two inputs to the MOC can increase cross-CF contrast in fluctuations (Farhadi *et al*., 2021). The two inputs to the MOC stage of the model were scaled to have approximately equal firing rates (the IC input was multiplied by 50), as otherwise the afferent input of the LSR fibers would dominate and limit modulation of OHC gain to enhance neural fluctuations (Figure 2). The MOC stage converted the input rates to a factor that modulated the cochlear gain. This conversion was based on an exponential relationship of firing rate to gain: the cochlear gain factor decreased exponentially as the combined input to the MOC stage increased. The final step in the MOC model stage was a low-pass filter with a time constant of 200 ms, chosen to approximate the overall time course of the MOC system.

For computational efficiency, a simple, bandpass modulation filter model (Mao et al., 2013) was used for the IC response that projected to the MOC in the efferent model (IC in Fig. 2e). Because the model of the IC that provided input to the MOC had a best modulation frequency of 64 Hz, regulation of cochlear gain was driven by both overall stimulus level (via the AN LSR input) and envelope fluctuations (via the IC input). This best modulation frequency of 64 Hz was selected as it was the mean of the distribution of best modulation frequencies observed by Kim et al. (2020) for rabbits. Then, for modeling listener thresholds, the final HSR AN response for both computational models was used as the input to a same-frequency inhibition-excitation (SFIE)

implementation of the IC (Nelson and Carney, 2004) with a best modulation frequency of 64 Hz. The SFIE model was used for the decision variable to avoid interference between "ringing" of the simple bandpass modulation filter at the end of the masker and the subsequent response to the signal (see Fig. 2e).

As illustrated in Fig. 2b, cochlear gain decreased after masker onset (due to high firing rates at stimulus onset for both the ANFs and IC). For the GN masker, this initial reduction in OHC gain was maintained throughout the duration of the masker and, due to the sluggishness of the MOC system, for a period after the offset of the masker. For the LFN masker, this initial reduction in OHC gain reduced over time (due to a reduction in firing rate from the IC). For the IC, these effects resulted in a greater response to the signal, relative to the masker rate, in the LFN condition. In the GN condition, the IC response during the masker was greater than in the LFN condition, and the signal response was decreased relative to the LFN condition due to decreased cochlear gain (Fig. 2b). Both higher masker response and lower signal response in the GN condition contributed to GN disruption in the model thresholds, as described further below.

One issue was the selection of characteristic frequencies (CFs) to include in estimating model thresholds. Presumably, participants used CFs tuned near the signal frequency of 4 kHz. Due to cochlear filtering of masker-frequency components, ANFs tuned to a masker-edge frequency will have slower fluctuations (for both masker types) than ANFs tuned to the masker center frequency. For the masker-edge CFs, there will be less IHC saturation and responsiveness to the signal stimulus. Here it was assumed that participants utilized activity in fibers with CFs that extended slightly beyond the bandwidth of the masker (3.9-4.1 kHz). Specifically, AN CFs of 3.6, 3.7, 3.8, 4, 4.2, 4.3, and 4.5 kHz were simulated. The IC stage of the model inherited these

CFs, and responses were summed across CFs after the IC stage before simulating listener thresholds.

Model IC responses were obtained for a 30-dB range of signal levels near an initial, rough approximation of model threshold. Signal levels were spaced 3 dB apart, and 50 trials were completed per signal level. Three independent simulations were used for the three-interval task, one of which was selected to include the signal tone. The silence preceding each interval was set to 1 second to allow the computational model to settle before stimulus onset. Under the assumption that—for the short 25-ms masker-signal delay—the participants listened from near the end of the masker to some time past the expected temporal position of the signal, the model-IC instantaneous firing rate was recorded from 375 ms after masker onset until at least 50 ms after the end of the probe tone (the decision-variable window). The start of the decision-variable window was delayed until 425 and 500 ms for the two longer masker-signal delays, respectively, and so the decision-variable window overlapped with the response to the masker only for the 25-ms masker-signal delay condition. The inclusion of the masker response in the decision variable for the shortest masker-signal delay conditions allowed the effect of listener uncertainty to be taken into account, and this measure of listener uncertainty contributed to elevating model thresholds to better approximate behavioral thresholds.

The interval with the highest maximum instantaneous rate during this timeframe was selected as the signal interval for that trial. The proportion correct was computed for each signal level, and a logistic function was then fit to each performance-intensity curve. Threshold was estimated as the level for which the curve intersected the 70.7% correct point. This process was repeated for each masker type, masker-signal delay, and participant group.

E. Analysis

All statistical models were computed using IBM SPSS version 27 or MATLAB (2021b) and the statistics and machine learning toolbox. Quiet conditions across participant groups (YNH, OMHL, OSNHL) were analyzed using a repeated measures analysis of variance. Post-hoc comparisons were completed using pairwise comparisons with false discovery rate adjustments (Glickman *et al*., 2014). To assess for differences in masked threshold by masker type (GN, LFN), masker-signal delay (25, 75, 150 ms), and hearing status (NH, SNHL), a linear-mixed effects model with random intercepts for each participant was conducted. Effect sizes (in dB), t-test values, and probability values are reported. Reference conditions were set to YNH, 25 ms masker-signal delay, and LFN. Using YNH as the reference group allowed the determination of effects of age and degree of hearing loss by comparing threshold for YNH to OMHL (effect of minimal hearing loss and age) and OSNHL (effect of mild-to-moderate hearing loss and age). Using the 25-ms masker-signal delay and LFN as the reference conditions allowed for the determination of whether GN disruption decreased from 25 to 75 ms or from 25 to 150 ms.

III. RESULTS

A. Absolute Thresholds

Figure 4 depicts detection thresholds in dB SPL. As expected, absolute thresholds (150 ms panel) were lowest for the YNH participants, with by progressively higher thresholds for the OMHL and OSNHL participants (df = 2,50, F = 194.2, p<.001). Post-hoc testing revealed that absolute thresholds were significantly higher for OMHL (p<.001, M=31.1, SD=6.2) and OSNHL

(p<.001, M=65.2, SD=9.0) participants than for YNH participants (M=21.3, SD=5.4). Detection thresholds were also significantly higher for OSNHL than for OMHL participants (p<.001).

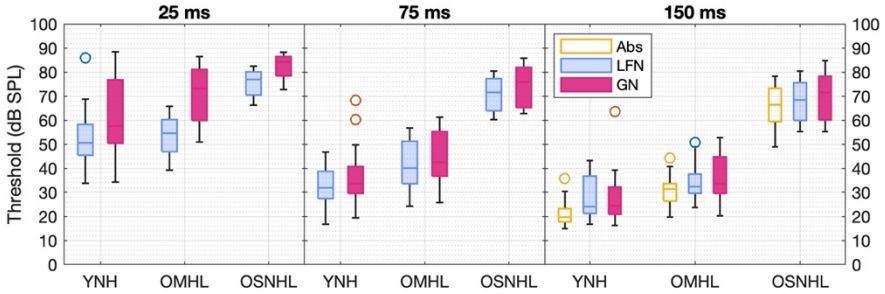

Fig. 4. (color online) Plots of threshold with the LFN and GN maskers for each delay time. Absolute (Abs) thresholds are in the 150 ms panel. Threshold decreased as delay time increased.

B. Masked Thresholds and GN Disruption

Consistent with prior work (Brennan *et al.,* 2015; Svec *et al.,* 2015, 2016) and as shown in Fig. 4, masked thresholds for all conditions were lowest for the YNH participants and was higher for OMHL and OSNHL participants. While not plotted, the amount of masking followed this same trend—being greatest for the YNH participants and progressively less for the OMHL and OSNHL participants. For the LFN masker, thresholds for the 25-ms masker-signal delay were significantly higher by 23 dB for the OSNHL than for the YNH participants (t=7.5, p<.001) but did not differ significantly for the OMHL and YNH participants (t=1.3, p=.700).

As hypothesized, threshold for the 25-ms masker-signal delay was significantly greater, for the YNH participant group, by 8.5 dB for the GN than for the LFN (t=5.1, p<.001), as also shown in Fig. 5. Consistent with the second hypothesis regarding expected effects of IHC saturation on GN disruption, GN disruption for the 25-ms masker-signal delay time was

significantly greater by 8.9 dB for the OMHL participants than for the YNH participants (t=3.5, *p*<.001). In contrast, GN disruption did not differ significantly between the YNH participants and the OSNHL participants (-1.5 dB, t=-0.6, *p*=.519). For the 75-ms masker-signal delay, GN disruption was statistically equivalent to that for the 25-ms masker-signal delay (-4.0 dB, t=-1.7, *p*=.093) for the YNH participants. GN disruption then decreased significantly, by 8 dB for the YNH participants, from the 25- to 150-ms masker-signal delay (t=-3.4, *p*<.001). The decrease in GN disruption from the 25- to the 75-ms masker-signal delay was significantly greater for the OMHL than for the YNH participants by 10.2 dB (t=-2.9, *p*=.004). Similarly, the decrease in GN disruption from the 25- to 150-ms masker-signal delay was significantly greater for the OMHL than for the YNH participants, by 7.3 dB (t=-2.1, *p*=.040). In contrast to the OMHL participants, the decreases in GN disruption from the 25-ms masker-signal delay to the 75- (t=0.3, *p*=.775) and 150-ms (t=0.9, *p*=.379) masker-signal delays were statistically equivalent for the YNH and OSNHL participants. Notice that variability in GN disruption, for the 25-ms masker-signal delay, was greatest for OMHL followed by YNH and OSNHL.

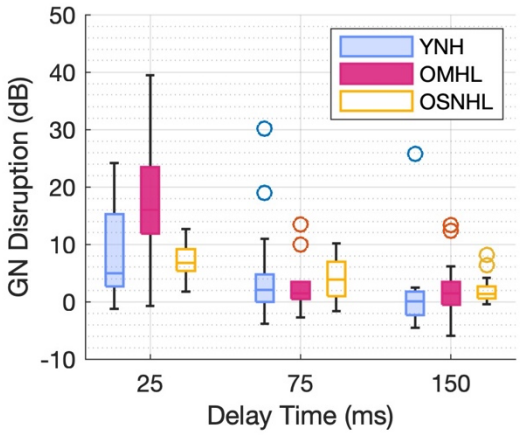

Fig. 5. (color online) Plot of GN disruption. For the 25-ms masker-signal delay, GN disruption was larger for the OMHL participants than for the other two groups.

In summary, GN disruption for the 25-ms masker-signal delay was significantly greater for OMHL than for YNH and OSNHL participants. Recovery from GN disruption was greater (steeper) for OMHL than for YNH participants, with similar GN disruption for the three participant groups for the two longest masker-signal delays.

C. Computational Models

Figure 6 plots the simulated OHC gain as a function of time for each masker, masker-signal delay, and participant group. For all three groups and both masker types, OHC gain decreased following masker onset. For the computational model of YNH, OHC gain initially decreased due to an increase in the rate of the IC and LSR inputs to the MOC (see Fig. 2). Following this abrupt gain decrease, OHC gain gradually increased over the remaining duration of each masker. For the YNH group, the model predicts that these participants would likely be operating in IHC saturation in the presence of a masker presented at 80 dB SPL. Due to IHC saturation, input fluctuations of the GN masker would be reduced. The reduction of masker envelope fluctuations at the level of the IC results in gradual OHC gain increase over the duration of each masker type. In contrast, for the computational model of OMHL, the model predicts that these participants would likely be operating below the saturation point of the IHC due to slight absolute threshold elevations, suggesting that robust envelope fluctuations from the GN masker would remain intact. This preservation of masker envelope fluctuations at the level of the IC results in gradual OHC gain decreases, as opposed to increases (YNH), over the duration of the GN masker. Consequently, there were larger differences in OHC gain over time between the two masker types (GN vs. LFN)

for the OMHL than for the YNH model. The OSNHL model predicts that the consequences of sensorineural hearing loss may lead to reduced OHC function, and therefore reduced OHC gain increases or decreases, as well as reduced possibilities for IHC saturation. Consequently, smaller changes in predicted OHC gain were observed between the two masker types for this group. Notice too that the differences in OHC gain across groups also occurred during the signal for the 25-ms masker-signal delay. For all groups, the difference in gain at the time of the signal between the two masker conditions decreased for the longer masker-signal delays.

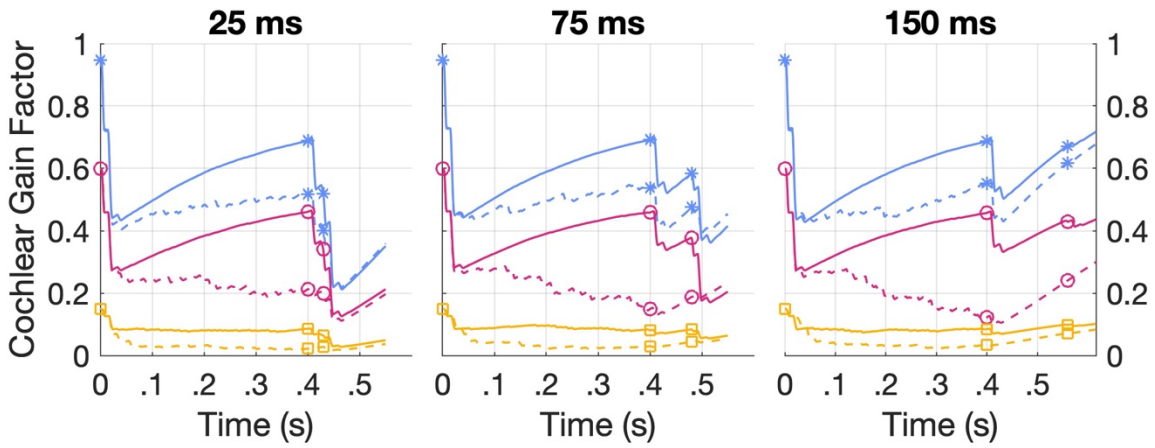

Fig. 6. (color online) Plot of OHC gain for each masker-signal delay. Responses are shown for one hair cell with CF = 4 kHz. Differences in OHC gain between GN (dashed lines) and LFN (solid lines) were greater for OMHL (circles/magenta) than for YNH (asterisks/blue) and OSNHL (squares/yellow). Symbols denote, in temporal sequence, start of the masker, end of the masker, and temporal center of the 10-ms signal. The signal level was set to 10 dB SPL above the predicted model threshold for the GN conditions (see Fig. 7).

Figure 7 illustrates the masked thresholds estimated from the computational model, with and without the efferent system. As expected, masked thresholds with the efferent system were higher (poorer) than without the efferent system. The increase in thresholds for the GN relative to

the LFN masker (i.e., GN disruption) was greater for the computational model when efferents were included. Note that the estimated thresholds were lower than the behavioral thresholds, with this difference largest for the YNH group. Figure 8 shows GN disruption estimated by the computational model, as well as measured behaviorally. Without the efferent system, GN disruption was minimal for YNH and OMHL. Starting with the 25-ms masker-signal delay condition, the estimates of GN disruption with the efferent system for YNH and OMHL groups increased by 4 and 18 dB, respectively, relative to the model without the efferent system. When the efferent system was included in the model, GN disruption was more similar in magnitude to the behaviorally measured GN disruption for all three participant groups. In addition, GN disruption estimated from the computational model with the efferent system was greatest for the OMHL group. GN disruption with the efferent system decreased for the two longer masker-signal delays and, with perhaps the exception of the 150-ms masker signal delay condition—better approximated GN disruption than the computation model without the efferent system.

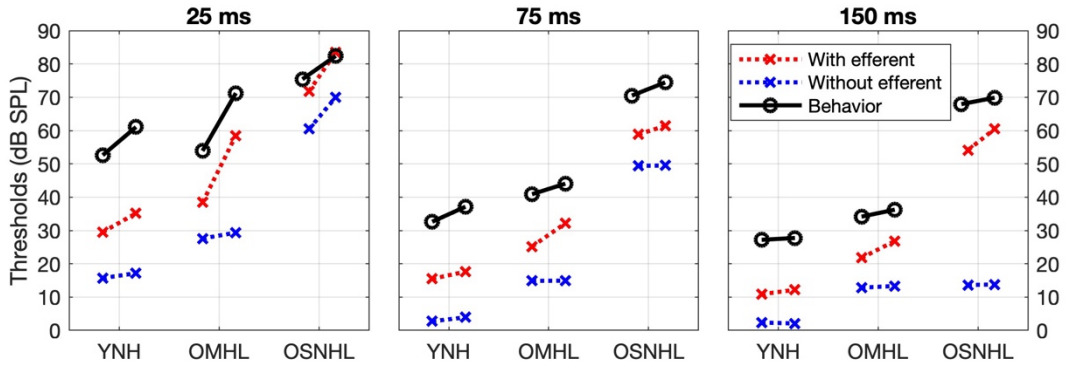

Fig. 7. (color online) Behavioral and model thresholds. Plots of mean behavioral and model predicted thresholds for YNH, OMHL, and OSNHL with and without the efferent system. The masker-signal delay condition is indicated above each plot.

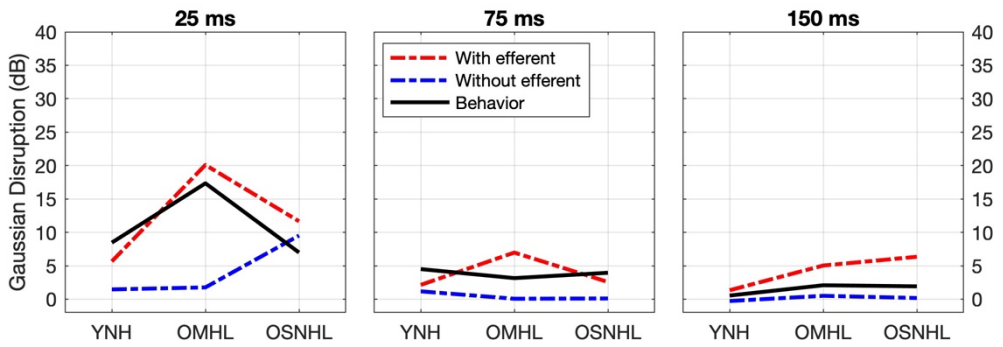

Fig. 8. (color online) Behavioral and model GN disruption. Plots of mean GN disruption for YNH, OMHL, and OSNHL with and without the efferent system. The masker-signal delay condition is indicated above each plot.

IV. DISCUSSION

A. Main Findings

Factors proposed to contribute to GN disruption include cochlear compression, listener uncertainty, inhibition within the auditory system, and the MOC efferent system. Because cochlear compression, inhibition, and MOC function vary with age and hearing status, this study was designed to: a) examine the contributions of each mechanism to GN disruption by comparing GN disruption for young participants with NH to older participants with minimal hearing loss or SNHL; and b) examine the extent to which a computational model of the IC and MOC could

account for the GN disruption observed in the behavioral results. The results suggest that the slightly elevated hearing thresholds of the OMHL participants may have made this group more susceptible than the other groups to the deleterious effects of masker envelope fluctuations. Specifically, greater GN disruption was observed for the 25-ms masker-signal delay for OMHL participants than for YNH and OSNHL participants and, based on the computational model, this greater GN disruption can be attributed to relatively reduced IHC saturation. For all three groups, GN disruption was reduced for the two longer masker-signal delays (75, 150 ms), and at these longer delays, significant differences in GN disruption between the groups were not found.

B. Cochlear Compression

Prior investigators have hypothesized that linearization of the basilar membrane associated with SNHL should result in greater effective amplitude fluctuations for GN, relative to a cochlea functioning normally (Moore *et al*., 1996; Svec *et al*., 2015). The greater effective magnitude of these fluctuations would likely cause increased difficulty for participants with SNHL, relative to the participants with NH, when attempting to detect a signal that follows a masker (Svec *et al*., 2016). If cochlear compression strongly contributed to GN disruption, then GN disruption should have been greater for the participants with SNHL than for the participants with NH. Instead, for the 25-ms masker-signal delay, GN disruption did not differ between the YNH and OSNHL participants and was *greatest* for the OMHL participants. While not statistically significant, these same trends were present in the GN disruption data of Svec *et al*. (2015). These results, at face value, do not support the argument that variations in cochlear compression across participants contributed toward differences in GN disruption. However, it is possible that GN disruption for the OSNHL participants was a consequence of a quasi-linearized basilar membrane response with

the absence of MOC efferent feedback. This notion is supported by the estimated GN disruption for the computational model without MOC efferent feedback. For this model, greater GN disruption (for the 25-ms masker-signal delay condition) was predicted for the OSNHL participants (9 dB) than for the YNH and OMHL participants (2 dB). This prediction of greater GN disruption for the OSNHL participants is consistent with a loss of OHC gain (and thereby compression) leading to larger fluctuations, and consequently, greater "modulation masking" by the GN masker.

C. Listener Uncertainty

While listener uncertainty, or confusion effects, have historically been observed at relatively brief masker-signal delays (< 20 ms; Moore 1981), Svec *et al*. (2016), showed significantly greater GN disruption for 10 OSNHL participants than for 9 YNH participants for a masker-signal delay of 75 ms, a finding that was not replicated here. While Svec and colleagues argued that listener uncertainty may have been greater for the OSNHL than for the YNH participants, due to the lack of significant differences between groups, the results of the current study do not support the notion GN disruption at longer masker-signal delays for older participants with minimal or greater hearing loss. The computational model, on the other hand, makes a case for the involvement of the efferent system in what has instead been traditionally attributed to listener uncertainty. The effect of different temporal window durations on GN disruption was informally examined. Variations in the temporal window for which the window length changed from including to not including the masker significantly decreased GN disruption. Otherwise, variations in the temporal window had at most a minimal effect on GN disruption. Possibly, the participants with less GN disruption used shorter temporal windows that did not include the

masker. Note that while listener uncertainty has been assessed using a diotic presentation of a masker as a comparison to an entirely monaural stimulus presentation, binaural interactions at the level of the MOC and IC (Park, 1998, 2004) should perhaps give investigators pause. If, for example, cochlear gain is driven by both contralateral and ipsilateral projections from the MOC, then changes in masked threshold due to the introduction of a contralateral masker may not reflect solely a reduction in listener uncertainty but could instead reflect reduced cochlear gain from the MOC.

D. Inhibition and Envelope Coding at the Inferior Colliculus

The computational model does not support the notion that offset-driven inhibition to the IC contributes strongly to GN disruption. When using pure-tone maskers, offset-driven inhibition to the IC has been argued to contribute to growth of masking for a 10-ms masker-signal delay (Salimi *et al.,* 2017). Salimi and colleagues used a similar computational model to the computational model without efferent of the current study. However, as indicated by the computational model results (see Fig. 8, 25-ms masker-signal delay condition), only approximately 2 dB of GN disruption can be attributed to inhibition for the YNH and OMHL participants without the inclusion of the efferent system. In contrast, mean behaviorally measured GN disruption was 8 dB for YNH participants and 17 dB for OMHL participants. Note that the best modulation frequency was centered at 64 Hz, which is lower than the mean modulation rate of the GN noise (98 Hz). While a modulation filter closer to the mean modulation rate of the GN noise could result in greater GN disruption, this is unlikely due to the use of a broad—but consistent with data from rabbits—modulation filter (Q=1; Kim *et al.*, 2020). When the computational model included efferents, GN disruption estimates were in good agreement with

behavioral results. Given that GN disruption is observable in the IC of rabbits with normal hearing for simultaneous tone-in-noise stimuli (Fan *et al.,* 2021), mechanisms other than offset-driven inhibition likely contribute to GN disruption. One limitation of the approach taken here is that variations in cell types or timing delays of inhibition were not examined, despite other cell types and time-delay values being physiologically plausible (Kim *et al.,* 2020). Note too that the computational model did not address changes in inhibition and envelope coding associated with age (Frisina and Rajan, 2005; Caspary *et al.,* 2008; Parthasarathy *et al.,* 2019), and thus, the authors cannot currently assess its contribution to GN disruption.

E. Role of MOC Efferent Feedback

Studies examining the physiological effect of MOC efferent feedback on firing rate within the IC provide supporting evidence that changes in rate within the IC may have contributed to GN disruption. The masker duration used here (400 ms) was sufficiently long to activate MOC efferent feedback (Cooper and Guinan, 2003) and the reduced a) GN disruption and b) forward masking for the longer masker-signal delays are consistent with the time course of OHC gain reduction following masker offset (Cooper and Guinan, 2003; Roverud and Strickland 2010; Guinan 2018). Note too that GN disruption, for some participants, was observed up to 150 ms following masker offset. Such an effect is consistent with previously estimated 4 – 8 dB of cochlear gain reduction for a relatively long precursor-signal delay of 120 ms for some participants (Roverud and Strickland 2010). Together, these results provide evidence that reduction in OHC gain associated with the efferent system could have contributed to the GN disruption that was observed for the 25-ms masker-signal delay and, for some participants, up to 150 ms.

Masked-threshold estimates from the computational model suggest there may be an influence of MOC efferent feedback on GN disruption. The computational model suggests that effects of masker type on firing rate within the IC without MOC efferent feedback are insufficient to explain GN disruption for individuals with normal hearing. For the 25-ms masker-signal delay condition, GN disruption estimated for the computation model without the MOC efferent system was only 2 dB for the 25-ms masker-signal delay, far less than the mean 8 and 17 dB measured for the YNH and OMHL participants, respectively. The addition of MOC efferent feedback to the computational model had the effect of reducing OHC gain within the model, which in turn, caused higher masked thresholds. More importantly, the amount of OHC gain reduction varied with masker type. There was a greater reduction in OHC gain for the GN than for the LFN masker. A greater reduction in gain likely occurred for the GN masker because the IC neurons that are excited by envelope fluctuations are assumed to excite MOC neurons, given that MOC neurons are also excited by envelope fluctuations (Gummer et al., 1988). As a result, for the YNH group in 25-ms delay condition, OHC gain was reduced for the GN masker relative to the LFN masker (see Figs. 2 & 6), and this difference in OHC gain contributed to an additional 4 dB, for 6 dB total, of GN disruption relative to the computational model without MOC efferent feedback. Note too that the computational model with the efferent system estimated decreased GN disruption for the two longer masker-signal delays and these decreases in GN disruption were generally consistent with the decrease in GN disruption observed from the participants. In contrast, the computational model without efferents predicted smaller changes in GN disruption for the longer masker-signal delays that were inconsistent with the participant data.

The computational model with the efferent system suggests that differences in the relative OHC gain over time between the three groups contributed to the differences observed in behavioral

GN disruption between groups. For the computational model of YNH, OHC gain initially decreased and then steadily increased over the duration of both maskers. In contrast, for the computational model of OMHL, OHC gain for the GN masker *decreased* over time. Due to a loss of IHC sensitivity and because OHC gain started out at a lower initial value (due to slight hearing threshold elevations), fluctuations within the IC were greater for the computational model for OMHL than for YNH. These more robust fluctuations caused OHC gain to *decrease* instead of increase over the duration of the masker. Consequently, a large GN disruption (for the 25-ms masker-signal delay) of 20 dB was predicted by the computational model, with 18 dB of the GN disruption attributable to the MOC efferent system. For OSNHL, the changes in OHC gain that occurred over time were largely reduced relative to the other two groups, owing to their SNHL. Consequently, there was less difference in OHC gain between the two masker types, and therefore, only 2 dB of GN disruption was attributable to MOC efferent feedback.

Across participants, GN disruption ranged from -4 to 40 dB and this variability in thresholds was largest for the OMHL participants. The results of the computational model suggest that this variability GN disruption can be attributed to variations in IHC saturation, which would be expected to increase with increasingly greater minimal hearing loss. The smaller variance in GN disruption for OSNHL can be attributed to their reduced likelihood of IHC saturation in response to either masker type.

The current study contributes to prior work attempting to relate perception to MOC efferent feedback (e.g., Winslow and Sachs, 1988; Jennings *et al.,* 2011; Wojtczak *et al.,* 2019) by comparing masked thresholds obtained with a computational model of the midbrain with MOC efferent feedback to behavioral measures of GN disruption and provided evidence suggesting that the MOC efferent system contributes to GN disruption. Such an approach was also used by

Jennings *et al*. (2011) to assess the role of MOC efferent feedback in overshoot, a phenomenon in which masked thresholds are higher for a signal near the onset and offset of a masker than for a signal near the temporal center of a masker. While the results of the computational model presented here indicate that modulation filtering, MOC efferent feedback, and IHC saturation provide plausible explanations for GN disruption, other aspects of auditory processing not assessed here could provide alternative explanations. For example, the effect of several model parameters was not assessed, including the spontaneous rate of the fiber used for the decision variable and the best modulation frequency of the IC. In addition, the computational model did not capture all aspects of auditory processing, such as sustained units (Krishna and Semple, 2000), the loss of auditory neurons associated with age (Makary *et al.,* 2011), or potential variations in the length of the temporal window across listeners or conditions. Possibly, some of these missing aspects of auditory processing in the computational model could account for 1) the better model thresholds as compared to behavioral thresholds and 2) individual differences in GN disruption.

CONCLUSIONS

- It appears that IC sensitivity to masker fluctuations and the concurrent decrease in OHC gain contributes to GN disruption for what has traditionally been attributed to listener uncertainty.
- Participants with minimal hearing loss may be more suspectable to GN disruption.
- A computational model of auditory processing in the IC with MOC efferent feedback indicated that increased saturation of inner hair cells, due to reduced efferent function, may have caused the relatively greater GN disruption observed for the participants with minimal hearing loss.

Declarations of interest: None.

AUTHORS CONTRIBUTIONS

MB and AS designed the research; MB performed the research; MB, BM, and AF analyzed the data and carried out computational modeling; MB and AS wrote the paper. All authors reviewed the paper and provided feedback.

ACKNOWLEDGEMENTS

Funding: This work was supported by the Nebraska Tobacco Settlement Biomedical Research Development Fund (MB) and the National Institutes of Health [010813 to LC, AF, & BM].

REFERENCES

American Speech Language Hearing Association. (2005). Guidelines for manual pure-tone threshold audiometry," Rockville, MD.

ANSI (2004). ANSI S3.6-2004, *Specification for audiometers*, (American National Standards Institute, New York).

Bernstein, L. R., and Trahiotis, C. (2018). "Effects of interaural delay, center frequency, and no more than "slight" hearing loss on precision of binaural processing: Empirical data and quantitative modeling," J. Acoust. Soc. Am. 144(1), 292-307.

Bidelman, G. M., Jennings, S. G., and Strickland, E. A. (2015). "PsyAcoustX: A flexible MATLAB(®) package for psychoacoustics research," Front. Psychol. 6, 1498.

Brennan, M. A., McCreery, R. W., and Jesteadt, W. (2015). "The influence of hearing-aid compression on forward-masked thresholds for adults with hearing loss," J. Acoust. Soc. Am. 138(4), 2589-2597.

Brennan, M., McCreery, R., Kopun, J., Lewis, D., Alexander, J., and Stelmachowicz, P. (2016). "Masking release in children and adults with hearing loss when using amplification," J. Speech Lang. Hear. Res. 59(1), 110-121.Brown, M. C. (2001). "Response adaptation of medial olivocochlear neurons is minimal," J. Neurophysiol. 86(5), 2381-2392.

Bruce, I. C., Sachs, M. B., and Young, E. D. (2003). "An auditory-periphery model of the effects of acoustic trauma on auditory nerve responses," J. Acoust. Soc. Am. 113(1), 369–388.

Buss, E., Hall III, J. W., and Grose, J. H. (2006). "Development and the role of internal noise in detection and discrimination thresholds with narrow band stimuli," J. Acoust. Soc. Am. 120(5), 2777-2788.

Carney, L. H. (2018). “Supra-threshold hearing and fluctuation profiles: Implications for sensorineural and hidden hearing loss,” J. Assoc. Res. Otolaryngol. 19(4), 331-352.

Carney, L. H., and McDonough, J. M. (2019). Nonlinear auditory models yield new insights into representations of vowels. Atten. Percept. Psychophys., 81(4), 1034-1046.

Caspary, D. M., Ling, L, Turner, J. G., and Hughes, L. F. (2008). “Inhibitory neurotransmission, plasticity and aging in the mammalian central auditory system,” J. Exp. Biol. 211(11), 1781-1791.

Cooper, N. P., and Guinan Jr, J. J. (2003). “Separate mechanical processes underlie fast and slow effects of medial olivocochlear efferent activity,” J. Physiol. 548(1), 307-312.

Darrow, K. N., Maison, S. F., and Lieberman, M. C. (2006). “Cochlear efferent feedback balances interaural sensitivity,” Nat. Neurosci. 9(12), 1474-1476.

Dau, T., Püschel, D., and Kohlrausch, A. (1996). “A quantitative model of the ‘‘effective’’ signal processing in the auditory system. II. Simulations and measurements,” J. Acoust. Soc. Am. 99(6), 3623-3631.

Derleth, R. P., Dau, T., and Kollmeier, B. (2001). “Modeling temporal and compressive properties of the normal and impaired auditory system,” Hear. Res. 159(1-2), 132-149.

Desloge, J. G., Reed, C. M., Braida, L. D., Perez, Z. D., and Delhorne, L. A. (2011). “Temporal masking functions for listeners with real and simulated hearing loss,” J. Acoust. Soc. Am. 130(2), 915-932.

DiGiovanni, J. J., Lynch, E. E., Nagaraj, N. K., and Ries, D. T. (2018). “Dominance of persistence over adaptation in forward masking,” Atten. Percept. Psychophys. 80(7), 1863-1869.

Fan, L., Henry, K. S., and Carney, L. H. (2021). “Responses to diotic tone-in-noise stimuli in the inferior colliculus: stimulus envelope and neural fluctuation cues,” Hear. Res. 409, 108328.

Farhadi, A., Jennings, S. G., Strickland, E. A., and Carney, L. H. (2021). A closed-loop gain-control feedback model for the medial efferent system of the descending auditory pathway. In *ICASSP 2021-2021 IEEE International Conference on Acoustics, Speech and Signal Processing (ICASSP)*, 291-295.

Faure, P. A., Fremouw, T., Casseday, J. H., and Covey, E. (2003). "Temporal masking reveals properties of sound-evoked inhibition in duration-tuned neurons of the inferior colliculus," J. Neurosci. 23(7), 3052-3065.

Frisina, R. D. and Rajan, R. (2005). "Inferior Colliculus: Aging and Plasticity," in *The Inferior Colliculus* (pp. 559-584). Springer.

Fuchs, P. A., and Lauer, A. M. (2019). "Efferent inhibition of the cochlea," Cold Spring Harb. Perspect. Med. 9(5), a033530.

Füllgrabe, C., Moore, B. C., and Stone, M. A. (2015). "Age-group differences in speech identification despite matched audiometrically normal hearing: contributions from auditory temporal processing and cognition," Front. Aging Neurosci. 6, 347.

Gifford, M. L., and Guinan Jr, J. J. (1983). "Effects of crossed-olivocochlear-bundle stimulation on cat auditory nerve fiber responses to tones," J. Acoust. Soc. 74(1), 115-123.

Glasberg, B. R., and Moore, B. C. (1990). "Derivation of auditory filter shapes from notched-noise data," Hear. Res., 47(1-2), 103-138.

Glickman, M. E., Rao, S. R., and Schultz, M. R. (2014). "False discovery rate control is a recommended alternative to Bonferroni-type adjustments in health studies," J. Clin. Epidemiol. 67(8), 850–857.

Guinan Jr, J. J. (2018). “Olivocochlear efferents: Their action, effects, measurement and uses, and the impact of the new conception of cochlear mechanical responses,” Hear. Res., 362, 38-47.

Gummer, M., Yates, G. K., & Johnstone, B. M. (1988). “Modulation transfer function of efferent neurones in the guinea pig cochlea,” Hearing research, 36(1), 41-51.

Hartmann, W. M., and Pumplin, J. (1988). “Noise power fluctuations and the masking of sine signals,” J. Acoust. Soc. Am. 83(6), 2277-2289.

Ibrahim, R. A., and Bruce, I. C. (2010). “Effects of peripheral tuning on the auditory nerve’s representation of speech envelope and temporal fine structure cues,” In *The neurophysiological bases of auditory perception* (pp. 429-438). Springer.

Jennings, S. G. (2021). “The role of the medial olivocochlear reflex in psychophysical masking and intensity resolution in humans: A review,” J. Neurophysiol. 125(6), 2279-2308.

Jennings, S. G., Heinz, M. G., and Strickland, E. A. (2011). “Evaluating adaptation and olivocochlear efferent feedback as potential explanations of psychophysical overshoot,” J. Assoc. Res. Otolaryngol. 12(3), 345-360.

Jennings, S. G., Strickland, E. A., and Heinz, M. G. (2009). “Precursor effects on behavioral estimates of frequency selectivity and gain in forward masking,” J. Acoust. Soc. Am. 125(4), 2172-2181.

Jesteadt, W., Bacon, S. P., and Lehman, J. R. (1982). “Forward masking as a function of frequency, masker level, and signal delay,” J. Acoust. Soc. Am. 71(4), 950-962.

Johannesen, P. T., Pérez-González, P., and Lopez-Poveda, E. A. (2014). “Across-frequency behavioral estimates of the contribution of inner and outer hair cell dysfunction to individualized audiometric loss,” Front Neurosci. 8, 214.

Joris, P., Schreiner, C. E., and Rees, A. (2004). "Neural processing of amplitude-modulated sounds," Physiol. Rev. 84(2), 541-577.

Kim, D. O., Carney, L., and Kuwada, S. (2020). "Amplitude modulation transfer functions reveal opposing populations within both the inferior colliculus and medial geniculate body," J. Neurophysiol. 124(4), 1198-1215.

Kohlrausch, A., Fassel, R., van der Heijden, M., Kortekaas, R., van de Par, S., Oxenham, A. J., and Puschel, D. (1997). "Detection of tones in low-noise noise: Further evidence for the role of envelope fluctuations," Acta. Acust. Acust. 83(4), 659-669.

Krishna, B. S., and Semple, M. N. (2000). "Auditory temporal processing: responses to sinusoidally amplitude-modulated tones in the inferior colliculus," J. Neurophysiol. 84(1), 255-273.

Kujawa, S. G., and Liberman, M. C. (2009). "Adding insult to injury: cochlear nerve degeneration after "temporary" noise-induced hearing loss," J. Neurosci. 29(45), 14077-14085.

Levitt, H. (1971). "Transformed up-down methods in psychoacoustics," J. Acoust. Soc. Am. 49(2B), 467-477.

Makary, C. A., Shin, J., Kujawa, S. G., Liberman, M. C., and Merchant, S. N. (2011). "Age-related primary cochlear neuronal degeneration in human temporal bones," J. Assoc. Res. Otolaryngol. 12(6), 711-717.

Mao, J., Vosoughi, A., and Carney, L. H. (2013). "Predictions of diotic tone-in-noise detection based on a nonlinear optimal combination of energy, envelope, and fine-structure cues," J. Acoust. Soc. Am. 134(1), 396-406.

Meddis, R., and O'Mard, L. P. (2005). "A computer model of the auditory-nerve response to forward-masking stimuli," J. Acoust. Soc. Am. 117(6), 3787–3798.

Moore, B. C. J. (1981). “Interactions of masker bandwidth with signal duration and delay in forward masking,” J. Acoust. Soc. Am. 70(1), 62-68.

Moore, B. C. J., Peters, R. W., and Glasberg, B. R. (1992). “Detection of temporal gaps in sinusoids by elderly subjects with and without hearing loss,” J. Acoust. Soc. Am. 92(4), 1923-1932.

Moore, B. C. J., Wojtczak, M., Vickers, D. A., 1996. “Effect of loudness recruitment on the perception of amplitude modulation,” J. Acoust. Soc. Am. 100(1), 481-489.

Mulders, W. H. A. M., and Robertson, D. (2000). “Evidence for direct cortical innervation of medial olivocochlear neurones in rats,” Hear. Res. 144(1-2), 65-72.

Neff, D. L. (1986). “Confusion effects with sinusoidal and narrowband noise forward maskers,” J. Acoust. Soc. Am. 79(5), 1519–1529.

Nelson, P. C., and Carney, L. H. (2004). “A phenomenological model of peripheral and central neural responses to amplitude-modulated tones,” J. Acoust. Soc. Am. 116 (4 Pt 1), 2173-2186.

Nelson, P. C., Smith, Z. M., and Young, E. D. (2009). “Wide-dynamic-range forward suppression in marmoset inferior colliculus neurons is generated centrally and accounts for perceptual masking,” J. Neurosci. 29(8), 2553-2562.

Nelson, P. C. and Young, E. D. (2010). "Neural correlates of context-dependent perceptual enhancement in the inferior colliculus," J. Neurosci. 19, 6577-6587.

Oxenham, A. J. (2001). “Forward masking: Adaptation or integration?” J. Acoust. Soc. Am. 109(2), 732-741.

Oxenham, A. J., and Moore, B. C. J. (1997). “Modeling the effects of peripheral nonlinearity in normal and impaired hearing,’’ in W. Jesteadt (Eds.), *Modeling sensorineural hearing loss* (pp. 273-288). Lawrence Erlbaum Associates.

Park, T. J. (1998). “IID sensitivity differs between two principal centers in the interaural intensity difference pathway: the LSO and the IC,” J. Neurophysiol. 79(5), 2416-2431.

Park, T. J., Klug, A., Holinstat, M., and Grothe, B. (2004). “Interaural level difference processing in the lateral superior olive and the inferior colliculus,” J. Neurophysiol. 92(1), 289-301.

Parthasarathy, A., Bartlett, E. L., and Kujawa, S. G. (2019). “Age-related changes in neural coding of envelope cues: Peripheral declines and central compensation,” Neurosci. 407, 21–31.

Plack, C. J., Drga, V., and Lopez-Poveda, E. A. (2004). “Inferred basilar-membrane response functions for listeners with mild to moderate sensorineural hearing loss,” J. Acoust. Soc. 115(4), 1684–1695.

Pumplin, J. (1985). “Low-noise noise,” J. Acoust. Soc. Am. *78*(1), 100–104.

Rabbitt, R. D., and Brownell, W. E. (2011). “Efferent modulation of hair cell function,” Curr. Opin. Otolaryngol. Head Neck Surg. 19(5), 376-381.

Roverud, E., and Strickland, E. A. (2010). “The time course of cochlear gain reduction measured using a more efficient psychophysical technique,” J. Acoust. Soc. Am. 128(3), 1203-1214.

Salimi N., Zilany M. S., and Carney L. H. (2017). “Modeling responses in the superior paraolivary nucleus: Implications for forward masking in the Inferior Colliculus,” J. Assoc. Res. Otolaryngol. 18(3), 441-456.

Savel, S., and Bacon, S. P. (2003). “Effectiveness of narrow-band versus tonal off-frequency maskers,” J. Acoust. Soc. Am. 114(1), 380-385.

Schofield, B. R. (2011). Central descending auditory pathways. In Auditory and vestibular efferents (pp. 261-290). Springer, New York, NY.

Sharf, B., Magnan, J., and Chays, A. (1997). “On the role of the olivocochlear bundle in hearing: 16 cases study,” Hear Res. 103, 101-122.

Smith, D. W., Turner, D. A., and Henson, M. M. (2000). "Psychophysical correlates of contralateral efferent suppression. I. The role of the medial olivocochlear system in "central masking" in nonhuman primates," J. Acoust. Soc. 107(2), 933-941.

Stone, M. A., Füllgrabe, C., Mackinnon, R. C., and Moore, B. C. (2011). "The importance for speech intelligibility of random fluctuations in steady background noise," J. Acoust. Soc. 130(5), 2874-2881.

Stone, M. A., Füllgrabe, C., and Moore, B. C. J. (2012). "Notionally steady background noise acts primarily as a modulation masker of speech," J. Acoust. Soc. 132(1), 317-326.

Svec, A., Dubno, J. R., and Nelson, P. B. (2015). "Effects of inherent envelope fluctuations in forward maskers for listeners with normal and impaired hearing," J. Acoust. Soc. Am. 137(3), 1336-1343.

Svec, A., Dubno, J. R., and Nelson, P. B. (2016). "Inherent envelope fluctuations in forward maskers: Effects of masker-probe delay for listeners with normal and impaired hearing," J. Acoust. Soc. Am. 139(3), 1195-1203.

Winslow, R. L., and Sachs, M. B. (1988). "Single-tone intensity discrimination based on auditory-nerve rate responses in backgrounds of quiet, noise, and with stimulation of the crossed olivocochlear bundle," Hear. Res. 35(2-3), 165-189.

Wojtczak, M., Klang, A. M., and Torunsky, N. T. (2019). "Exploring the role of medial olivocochlear efferents on the detection of amplitude modulation for tones presented in noise," J. Assoc. Res. Otolaryngol. 20(4), 395-413.

Wojtczak, M. and Oxenham, A. J. (2010). "Recovery from on- and off-frequency forward masking in listeners with normal and impaired hearing," J. Acoust. Soc. Am. 128(1), 247-256.

Ye, Y., Machado, D. G., and Kim, D. O. (2000). "Projection of the marginal shell of the anteroventral cochlear nucleus to olivocochlear neurons in the cat," J. Comp. Neurol. 420(1), 127-138.

Zilany, M. S., & Bruce, I. C. (2007). Representation of the vowel /ε/ in normal and impaired auditory nerve fibers: model predictions of responses in cats. J. Acoust. Soc. Am., 122(1), 402-417.

Zilany, M. S. A., Bruce, I. C., Nelson, P. C., and Carney, L. H. (2009). "A phenomenological model of the synapse between the inner hair cell and auditory nerve: Long-term adaptation with power-law dynamics," J. Acoust. Soc. Am. 126(5), 2390–2412.

Zilany, M. S. A., Bruce, I. C., and Carney, L. H. (2014). "Updated parameters and expanded simulation options for a model of the auditory periphery," J. Acoust. Soc. Am. 135(1), 283–286.

Zurek, P. M., and Durlach, N. I. (1987). "Masker-bandwidth dependence in homophasic and antiphasic tone detection," J. Acoust. Soc. Am. 81(2), 459-464.